Journal of Simulation & Analysis of Novel Technologies in Mechanical Engineering
10 (4) (2017) 0033~0048
HTTP://JSME.IAUKHSH.AC.IR
ISSN: 2008-4927

Free Vibration Analysis of Sandwich Micro Beam with Piezoelectric Based On Modified Couple Stress Theory and Surface Effects

Mohamad Khaje khabaz, S. Ali Eftekhari*, Mohamad Hashemian

Department of Mechanical Engineering, Khomeinishahr Branch, Islamic Azad University, Isfahan, 84175-119, Iran

Corresponding Author: a.eftekhari@iaukhsh.ac.ir

(Manuscript Received --- 14 Jan. 2018; Revised --- 12 May 2018; Accepted --- 11 June 2018)

Abstract

In this paper, free vibration analysis of sandwich micro beam with piezoelectric layers based on modified couple stress and surface elasticity theories are investigated. The Hamilton's principle is employed to derive the sandwich micro beam with piezoelectric based on modified couple stress theory incorporating with Gurtin- Murdoch surface theory. Generalized differential quadrature method is used to discretize the partial differential equation into the ordinary differential equation. The effect of various parameters such as thickness to material length scale parameter ratio, surface residual stress, Young's modulus of surface layer, surface mass density and surface piezoelectric constant are investigated by comparing the results obtained using the modified couple and classical theories. Numerical results of this problem evaluate the effect of micro length scale parameters on natural frequency. The results show that surface parameter effects are significant when the model is small, but can be neglected with increasing model size.

Keywords: Micro-beam, Modified couple stress elasticity theory, Gurtin- Murdoch surface theory, Free vibration analysis

1- Introduction

Nowadays, many researchers have focused on material behavior at the field of micro and nano electro-mechanical systems (MEMS and NEMS). MEMS and NEMS have an important role in different mechanical engineering applications such as atomic forces micro-scopes (AFMS), micro-switches, micro and nano sensors and actuators, micro rate gyros and micro flexible joints. Experimental researches have illustrated when the length characteristic is on the order of microns, size effect must be taken into account in mechanical behavior of micro scale structure. Fleck et al. [1] studied mechanical behavior of thin micro copper wire. Their experiment showed that shear strength increased three times as the wire diameter decreased from 170μm to 12μm. Stolken and Evasns [2] found that fluctuation of beam thickness had a great effect on normalized bending hardening. The size dependence of deformation observed in micro and nano mechanical behaviors showed that classical theory

cannot interpret accurately because of lacking in intrinsic length scales. Non classical continuum theories considering the size effect have been presented to predict static and dynamic behaviors of micro and nano scale. Therefore, many theories which are more accurate and reliable results of mechanical behavior such as nonlocal elasticity [3], couple stress theory [4], modified couple stress [5] and strain gradient theory [6] have been already introduced.

Modified couple stress and strain gradient are two theories which have been developed using higher order nonlocal theories considering length scale parameters. Many researches have been carried out to analyze the linear and nonlinear behavior of micro and nano beams model based on introduced theories. Young et al. [5] presented modified couple stress theory which involves material length scale. Lam et al. represented the strain gradient theory including three material length scale parameters by applying dilatation gradient, deviatoric gradient and symmetric rotation gradient tensors.

Afterwards, the analysis of mechanical behavior of micro-beams based on modified couple stress and strain gradient theories have received considerable attention by researchers. Zhao and Park [7] analyzed static deflection of Euler-Bernoulli micro-beam with different boundary conditions based on modified couple stress theory. Good agreement has been achieved between their provided results and experimental data. Kong et al. [8] calculated the natural frequency of Euler-Bernoulli micro-beam based on modified couple stress theory. In the mentioned research, the moment of inertia was neglected and analytical solution was employed to find natural frequency problem and Alashti et al. [9] represented size-dependent behavior of micro-beam by employing the couple stress theory to study static and free vibration problem. The natural frequency results are compared with classical beam theory. They results showed that predicted deflection by the aforementioned method is lower than of the classical theory. Dynamical behavior of geometrical imperfect micro-beam developed by Farokhi et al. [10] based on modified couple stress. They used Galerkin method to discretize equation of motion and nonlinear frequency behavior was evaluated. Buckling analysis of axially micro-beam based on modified and strain gradient theory were extended by Akgöz and Civalek [11]. They investigated critical buckling load under different type of boundary conditions. Kong et al. [12] carried out an analytical approach for static and dynamic analysis of micro cantilever beam using strain gradient theory. In other attempts, static, buckling and free vibration analysis of micro-beam utilized by Lingan et al. [13]. It can be seen from their results that the frequency decreases with increasing thickness. Also, influence of the thickness and Poisson's ratio on frequency are examined. It should be mentioned that determining material length scale parameter is still a challenging issue and there are some ambiguities in this research field. Lazopoulos and Lazopoulos [14] demonstrated bending and buckling of thin elastic beam. By the strain gradient theory, they deduced that the dependence of the cross-section area increases when the beam thickness decreases. This effect is attributed to the thin beam stiffness increase.

As a new field in very small scale structures, researchers considered micro scale beam integrated with piezoelectric layer. Piezoelectric layers are widely used in flexible structures as sensors and actuators. These materials are used for vibration suppression, shape control and active damping. The finite element model developed by Trindade and Benjeddou [15] to evaluate vibrational response of classical sandwich beam including dynamic piezoelectric actuator and sensor. Stability of transvers motion analyzed by Ghaznavi et al. [16] for cantilever micro-beam integrated with sensor and actuator piezoelectric layers. Sahmani et al. [17] elucidated dynamic stability of micro-beam actuated by piezoelectric voltage using strain gradient theory. Moreover, they compared critical piezoelectric voltages including various values for length scale parameter with those predicted by the classical theory. Ghorbanpour Arani et al. [18] discussed vibration of coupled piezoelectric nano-beams enclosing elastic medium which is simulated as Pasternak foundation. They derived the equations of motion using the strain gradient theory and Hamilton's principle. They employed DQM to solve the partial equation of motion. Most of these studies have performed their models without considering surface stress effect. Surface stress is one of the most important effects which ignoring it may cause some unusual behavior in micro and nano structures. A continuum surface energy theory has been introduced by Gurtin and Murdoch [19]. Stability of electromechanical bridges using Gurtin-Murdoch elasticity theory have conducted by Fu and Zhang [20]. Mohammadimehr et al. [21] have applied Gurtin–Murdoch elasticity theory to demonstrate the impact of surface energy on free vibration and bending on nonlocal single-layer graphene sheet.

In the present study, a cantilever sandwich piezoelectric micro-beam has been analyzed based on modified couple stress and Gurtin-Murdoch surface elasticity to calculate free vibration behaviors. Most studies in the field of micro and nano beam have focused on higher order elasticity theories. Hence, surface elasticity theory and modified couple stress are considered in the developed model. The governing equations of motion are obtained by the Hamilton's principle and then discretized using GDQM. Finally, the effects of small length scale, geometric properties and surface parameters on the vibrational behavior are studied in detail.

2- Governing equations of motion

Fig. 1 shows a schematic of micro cantilever beam integrated with piezoelectric layers. In this model, length and width of micro-beam are L and b, respectively. Also, h_b and h_p denote two thickness parameters associated with the bulk and piezoelectric thickness, respectively.

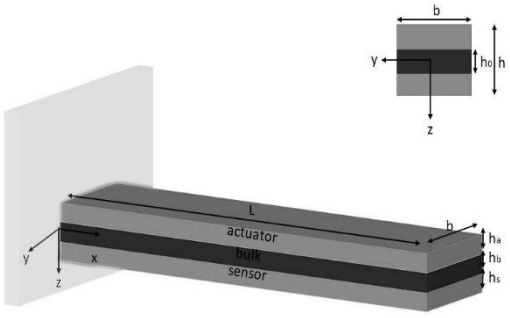

Fig. 1- Schematic of micro beam with piezoelectric layers

The displacement field of an Euler-Bernoulli beam is stated as [22]:

$$U_1 = -Z\frac{\partial w(X,t)}{\partial X} \quad (1)$$

$$U_2 = 0$$

$$U_3 = w(X,t)$$

where U_1, U_2 and U_3 are displacements in X, Y and Z direction, respectively. The strain energy based on modified couple stress theory and electrical field is defined as [23]:

$$U = \int_{\Omega} (\sigma_{ij}\, \varepsilon_{ij} + m_{ij} x_{ij} - D_i E_i) dV \quad (2)$$

where σ_{ij} and ε_{ij} are Cauchy stress and strain tensors which are defined as Eqs. (3) and (4), respectively [18].

$$\sigma_{ij} = \lambda \delta_{ij} \varepsilon_{mm} + 2\mu \varepsilon_{ij} - e_{nij} E_n \quad (3)$$

$$\varepsilon_{ij} = \frac{1}{2}\left(u_{i.j} + u_{j.i}\right) \quad (4)$$

In which λ and μ are the Lame constants, e and $\delta_{ij}$are the piezoelectric coefficient and kronecker delta. Also m_{ij}, x_{ij} , D_i and E_i denote the deviatoric part of couple stress tensor, symmetric curvature tensor, electrical displacement and electrical field, respectively which are given as Eqs. (5)-(8) [18]:

$$m_{ij} = 2\mu l_2^2 \chi_{ij} \quad (5)$$

$$\chi_{ij} = \frac{1}{2}\left(\theta_{i,j} + \theta_{j.i}\right) \quad (6)$$

$$D_i = e_{imn} \varepsilon_{mm} + \epsilon_{im} E_m \quad (7)$$

$$E_i = -\Phi_{,i} \quad (8)$$

where θ, ϵ, $\Phi_{,i}$, μ and l_2 are the infinitesimal rotation vector, the dielectric permittivity constant, the electric potential, shear modulus and length scale parameter associated with symmetric rotation gradients, respectively. The classical model will be achieved with l_2 equal to zero. The Rotation vector is considered as Eq. (9) [17]:

$$\theta_i = \frac{1}{2} curl\left(u_{i.j}\right) \quad (9)$$

The electrical potential distribution in the thickness direction of the piezoelectric micro layer is assumed as Eq. (10) [18]:

$$\Phi^{(p)}(x, z, t) = -\cos(\beta z)\phi\,(x, t) + \frac{2zV_0}{h^{(p)}} \quad (10)$$

where $\beta = {}^{\pi}/_{h_p}$ and V_0 is the external electric voltage. According to Gurtin-Murdoch continuum mechanics theory, the strain energy in the surface layer can be explained as [24, 25]:

$$U_s = \frac{1}{2}\int_0^L \oint_{\partial A} (\tau_{ij}\, \varepsilon_{ij} + \tau_{ni} u_{n,i}) \quad (11)$$

where τ^s is the residual surface stress under uncertain condition. Also $\tau_{\alpha\beta}$ is the in-plane components of surface stress tensor which can be explained as Eqs. (12) and (13) [26].

$$\tau_{\alpha\beta} = \mu^s\left(u_{\alpha,\beta} + u_{\beta,\alpha}\right) + (\lambda^s + \tau^s) u_{k,k} \delta_{\alpha\beta} + \tau^s(\delta_{\alpha\beta} - u_{\beta,\alpha}) \quad (12)$$

$$\tau_{n\alpha} = \tau^s(u_{n,\alpha}) \quad (13)$$

λ^s and μ^s are surface elastic constants which are assumed as follows [23]:

$$\lambda^s = \frac{E^s \upsilon^S}{(1 + \upsilon^S)(1 - 2\upsilon^S)} \quad (14)$$

$$\mu^s = \frac{E^s}{2(1 + \upsilon^S)} \quad (15)$$

where υ^S and E^s are Poisson's ratio and Young's modulus, respectively.

Substituting relations (3)-(15) in Eq. (2), after some mathematical elaboration, the strain energies of micro beam integrated with piezoelectric layers and surface strain energies can be expressed as Eqs. (16) and (17):

$$U = U^{(b)} + U^{(p)} \tag{16}$$
$$= \frac{1}{2}\int_0^L \int_A \left[EZ^2 \left(\frac{\partial^2 w}{\partial x^2}\right)\left(\frac{\partial^2 w}{\partial x^2}\right) + \mu^{(b)} l_2^2 \left(\frac{\partial^2 w}{\partial x^2}\right)\left(\frac{\partial^2 w}{\partial x^2}\right) + 2E^{(p)} Z^2 \left(\frac{\partial^2 w}{\partial x^2}\right)\left(\frac{\partial^2 w}{\partial x^2}\right) + 2e_{31} Z \left(\frac{\partial \Phi^{(P)}}{\partial z}\right)\left(\frac{\partial^2 w}{\partial x^2}\right) + 2\mu^{(p)} l_2^2 \left(\frac{\partial^2 w}{\partial x^2}\right)\left(\frac{\partial^2 w}{\partial x^2}\right) + 2e_{31} Z \left(\frac{\partial^2 w}{\partial x^2}\right)\left(\frac{\partial \Phi^{(P)}}{\partial z}\right) + 2\epsilon_{33} \left(\frac{\partial \Phi^{(P)}}{\partial z}\right)\left(\frac{\partial \Phi^{(P)}}{\partial z}\right)\right] dA dx$$

$$U_s = U_s^{(b)} + U_s^{(p)} \tag{17}$$
$$= \frac{1}{2}\int_0^L \oint_{\partial A} \left[\left(\tau_s^{(b)} + E_s^{(b)} \varepsilon_{11}^s\right)\left(-z\frac{\partial^2 w}{\partial x^2}\right) + \tau_s^{(b)} \left(\frac{\partial w(x)}{\partial x}\right)^2 + 2\left(\tau_s^{(p)} + E_s^{(p)} \varepsilon_{11}^s - e_{31}^{s(p)} E_3\right)\left(-z\frac{\partial^2 w}{\partial x^2}\right) + 2\tau_s^{(p)} \left(\frac{\partial w(x)}{\partial x}\right)^2\right] ds\, dx$$

Kinetic energies of bulk model and piezoelectric layers can be found as Eq. (18) and (19) [18]:

$$T^{(b)} = \tag{18}$$
$$\frac{1}{2}\int_0^L \left[I_0^{(b)} \left(\frac{\partial w}{\partial t}\right)^2 + I_2^{(b)} \left(\frac{\partial^2 w}{\partial x \partial t}\right)^2\right] dx$$

$$T^{(p)} \tag{19}$$
$$= \frac{1}{2}\int_0^L \left[I_0^{(p)} \left(\frac{\partial w}{\partial t}\right)^2 + I_2^{(p)} \left(\frac{\partial^2 w}{\partial x \partial t}\right)^2\right] dx$$

Also $I_0^{(b)}$, $I_2^{(b)}$, $I_0^{(p)}$and $I_2^{(p)}$ can be obtained as Eqs. (20) and (21), respectively:

$$I_0^{(b)} = \int_{A^{(b)}} \rho_B \, dA^{(b)} \tag{20}$$
$$I_2^{(b)} = \int_{A^{(b)}} \rho_B Z^2 \, dA^{(b)}$$

$$I_0^{(p)} = \int_{A^{(p)}} \rho_P \, dA^{(p)} \tag{21}$$
$$I_2^{(p)} = \int_{A^{(p)}} \rho_P Z^2 \, dA^{(p)}$$

where ρ_B and ρ_P are density of bulk and piezoelectric, respectively.

Π is the total potential energy of model which can yield form Eq. (22):

$$\Pi = U^{total} - T^{total} \tag{22}$$

where

$$U^{total} \tag{23}$$
$$= U^{(b)} + U^{(p)} + U_s^{(b)} + U_s^{(p)}$$
$$T^{total} = T^{(b)} + T^{(p)} \tag{24}$$

where $U^{(b)}$, $U^{(p)}$, $U_s^{(b)}$ and $U_s^{(p)}$are the strain energies of bulk, piezoelectric layer and surface strain energies of bulk and piezoelectric, respectively. Substituting Eqs. (23) and (24) into Hamilton's principle and variational method given by:

$$\delta \int_{t_1}^{t_2} (U^{total} - T^{total})\, dt = 0 \quad (25)$$

yields the following partial differential governing equations of motion for micro-beam integrated with piezoelectric layers as follows:

$$\begin{aligned}
&\delta w: (A_1 + A_2 + A_3 + A_{12} + A_{13} \quad (26)\\
&+ A_{14} + B_1^S + B_4^S + B_6^S + B_8^S\\
&+ B_{10}^S + B_{14}^S + B_{15}^S)\left(\frac{\partial^4 w}{\partial x^4}\right)\\
&+ (A_4 + B_2^S + B_5^S + B_7^S)\\
&\left(\frac{\partial^2 \phi^{(a)}}{\partial x^2}\right)\\
&+ (A_5 + B_{11}^S + B_{13}^S + B_{16}^S)\\
&\left(\frac{\partial^2 \phi^{(S)}}{\partial x^2}\right) - (B_3^S + B_9^S + B_{12}^S)\\
&\left(\frac{\partial^2 w}{\partial x^2}\right) + (A_6)\left(\frac{\partial^4 w}{\partial x^2 \partial t^2}\right)\\
&+ (A_7)(\frac{\partial^2 w}{\partial t^2}) = 0\\
&\delta \phi^{(a)}: (A_8 + B_5^S + B_7^S + B_2^S)\\
&\left(\frac{\partial^2 w}{\partial x^2}\right) + (A_9)\left(\phi^{(a)}\right) = 0\\
&\delta \phi^{(s)}: (A_{10} + B_{16}^S + B_{11}^S + B_{13}^S)\\
&\left(\frac{\partial^2 w}{\partial x^2}\right) + (A_{11})\left(\phi^{(s)}\right) = 0
\end{aligned}$$

in which $A_i\ (i = 1, 14)$ and $B_i^s\ (i = 1, 16)$ are coefficients of relations, defined in Appendix. The boundary conditions of micro cantilever beam are obtained from Eq. (27):

$$w(0) = 0 \quad (27)$$

$$\frac{\partial w(0)}{\partial x} = 0$$

$$\frac{\partial^2 w(L)}{\partial x^2} = 0$$

$$\frac{\partial^3 w(L)}{\partial x^3} = 0$$

3- Solution and discretization

In order to discretize the governing equations, the generalized differential quadrature method (GDQM) was utilized. In this method, derivative of a function assumed as weighted linear summation of function values at intended grid points along the coordinate direction. Therefore, the partial differential is converted to a set of algebraic equations**.** The partial derivatives of a function f at a point x_i can be defined as:

$$f^{(r)}(x_i) = \sum_{i=1}^{N} C^{(n)} f(x_i)\,, \quad i = 1, 2, \dots, N \quad (28)$$

where C_{ij}, are weighting coefficients, (n) and (r) are the number of grid points and order of derivation, respectively. First derivative of weighting coefficients can be achieved as Eq. (29).

$$C_{ij}^{(1)} = \begin{cases} \prod_{k=1, k\neq i}^{N} (x_i - x_k) \Big/ \prod_{k=1, k\neq i}^{N} (x_j - x_k) \\ \sum_{k=1, k\neq i}^{N} \frac{1}{(x_i - x_k)} \end{cases} \quad \begin{matrix} \\ (i = j) \end{matrix} \quad (29)$$

The weighting coefficients of higher order derivatives are given by:

$$C_{ij}^{(2)} = \sum_{K=1}^{N} C_{ik}^{(1)} C_{kj}^{(1)} \quad (30)$$

$$C_{ij}^{(3)} = \sum_{K=1}^{N} C_{ik}^{(1)} C_{kj}^{(2)} = \sum_{K=1}^{N} C_{ik}^{(2)} C_{kj}^{(1)}$$

$$C_{ij}^{(4)} = \sum_{K=1}^{N} C_{ik}^{(1)} C_{kj}^{(3)} = \sum_{K=1}^{N} C_{ik}^{(3)} C_{kj}^{(1)}$$

Considering the grid points are distributed by shifted Chebyshev–Gauss–Lobatto grid points as follows [27]:

$$x_i = \frac{1}{2}\left[1 - \cos\left(\frac{(i-1)\pi}{N-1}\right)\right] \quad (31)$$

$$i = 1, 2, \ldots N$$

Employing the GDQM, discretized governing differential equations can be derived as following:

$$\delta w: (A_1 + A_2 + A_3 + A_{12} + A_{13} + A_{14} + B_1^S + B_4^S + B_6^S + B_8^S + B_{10}^S + B_{14}^S + B_{15}^S) \sum_{1}^{N} A_{ik}^{(4)} w_k + (A_4 + B_2^S + B_5^S + B_7^S) \sum_{1}^{N} A_{ik}^{(2)} \phi_k^{(a)} + (A_5 + B_{11}^S + B_{13}^S + B_{16}^S) \sum_{1}^{N} A_{ik}^{(2)} \phi_k^{(s)} + (A_6) \sum_{1}^{N} A_{ik}^{(2)} w_k \left(\frac{\partial^2 w}{\partial t^2}\right) + (A_7)\left(\frac{\partial^2 w}{\partial t^2}\right) = 0 \quad (32)$$

$$\delta\phi^{(a)}: (A_8 + B_5^S + B_7^S + B_2^S) \sum_{1}^{N} A_{ik}^{(2)} w_k + (A_9)\left(\phi^{(a)}\right) = 0$$

$$\delta\phi^{(s)}: (A_{10} + B_{16}^S + B_{11}^S + B_{13}^S) \sum_{1}^{N} A_{ik}^{(2)} w_k + (A_{11})\left(\phi^{(s)}\right) = 0$$

Equation (32) can be rewritten in the matrix form as:

$$[M]\{\ddot{X}\} + [K]\{X\} = \{0\} \quad (33)$$

in which $[M]$ and $[K]$ are the mass and the global stiffness matrices, respectively. In order to investigate free vibration, the formulation of micro-beam can be obtained as:

$$[K]\{X\} = \omega^2[M]\{X\} \quad (34)$$

By solving Eq. (34), the natural frequencies and vibrational behavior of model can be extracted.

4- Results and discussion

In this section, the effect of various parameters such as thickness to material length scale parameter ratio, surface residual stress, Young's modulus of surface layer, surface mass density and surface piezoelectric constant of integrated cantilever micro beam based on modified couple stress continuum theory are investigated.

The mechanical and geometrical properties of bulk and piezoelectric layers are considered as Table.1 [17]. It is assumed that the micro-beam consists of silicon material properties with PZT-4

piezoelectric integrated to the lower and upper surfaces of bulk.

Table 1- The geometric and material constant of the micro-beam and piezoelectric layer.

Parameters	Bulk	Piezoelectric layer
Thickness(μm)	3	3
Length(μm)	450	450
Width(μm)	50	50
Young's modulus (Gpa)	210	64
Mass density(Kg/m^3)	2331	7500
Poisson's ratio	0.24	0.27
$e_{31}(C/m^2)$	-	-10
$\in_{33}(C^2/m^2\,N)$	-	1.0275×10^{-8}
$l\ (\mu m)$	17.6	17.6

Fig. 2 shows the GDQ convergence diagram and illustrates comparison results of classical and couple stress theories for different number of grid points on the convergence and accuracy of natural frequency. It can be concluded that by increasing the number of grid points, the accuracy of the natural frequency increases and the convergence of results happen for 13 grid points and higher.

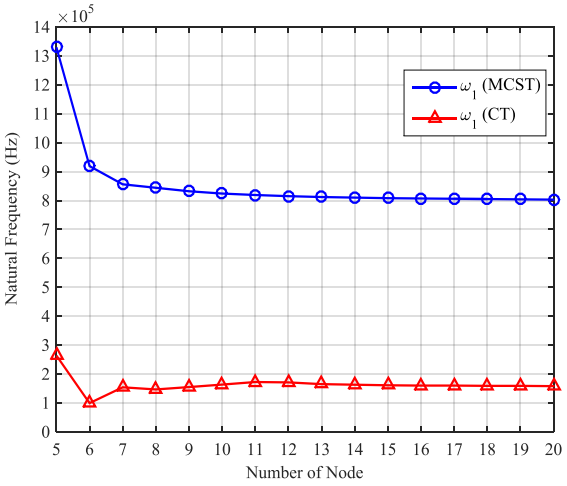

Fig. 2- Comparison between the classical and modified couple tress theories convergence of natural frequency with respect to the number of sample grid points

4-1- Validation

Several comparisons are applied to verify the accuracy and compatibility of the present method for analyzing the frequency response. Since no published literature is available for validating the results directly, the frequency results are compared with simple micro-beam offered by Kong et al. [12] in which piezoelectric layers are ignored. The mechanical and geometrical properties of the structure are considered the same as presented values by Kong et al. [8]. Fig. 3 shows the comparison results of Kong et al. [8] and present work. In this figure, the effect of thickness on natural frequencies based on classical and modified couple stress has been plotted. It is clearly shown that excellent agreement is achieved, according to the compare with the analytical solution presented by Zhao.

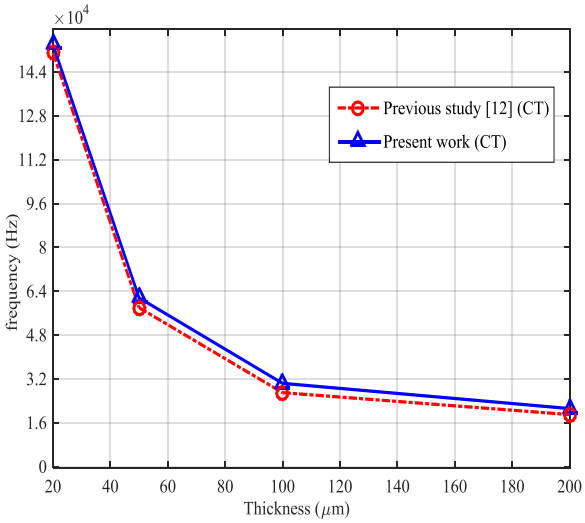

Fig. 3- The comparison between the results of present study and [12] for effect of thickness on the variation of the first natural frequency

4-2- Length parameters effects

Fig. 4 shows the variation of natural frequency versus thickness in different beam lengths. The thickness of each layer including bulk and piezoelectric is assumed to be constant in order to investigate the natural frequency. Different length scales have been compared in this figure where the value of natural frequency for L=5H is larger than the others. The lowest curve introduces L=20H where the natural frequency has the minimum value

respect the other cases. Then, it can be said that in the same values of thickness parameters, the natural frequency of local system is decreased where the values of beam length increases. As illustrated, the maximum frequency is achieved aspect ratio variation of the micro-beam model becomes larger and the thickness value is 3- 12 μm.

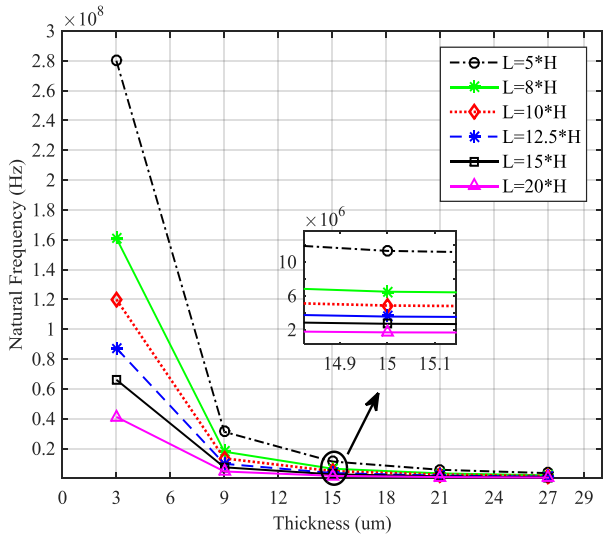

Fig. 4- Effect of natural frequency on the variation of the thickness of micro cantilever beam with different length scale parameters.

Fig. 5 depicts the effect of width to thickness ratio variation between CT and MCST cantilever sandwich micro-beam with piezoelectric layers versus aspect ratio on the first natural frequency. It is clearly observed that the natural frequency increases in MCST. This is due to the fact that, the stiffness matrix of MCST contains material length scale parameter, which increases the natural frequency of MCST micro-beam. Moreover, it is clearly seen that when the width to thickness ratio increases, the value of natural frequency decreases.

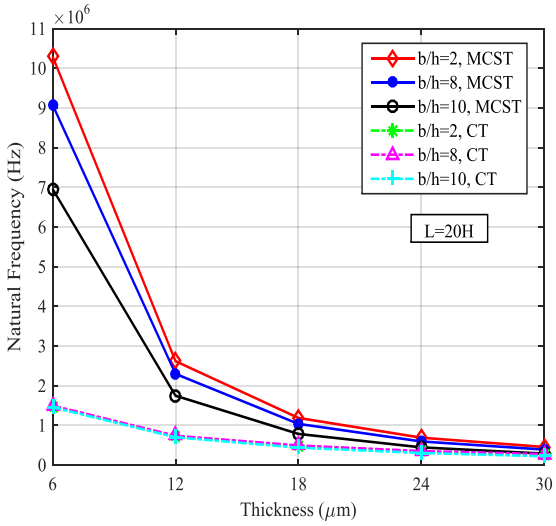

Fig. 5- Width to thickness ratio variation effect between CT and MCST

The effects of the micro-scale parrameter l_2 on natural frequency and size-dependency are indicated in Figs. 6 and 7. Different length scale parameter values of l_2 are evaluated in those figures. Fig. 6 is the distribution of the first natural frequency of the sandwich micro-beam in terms of the different size-dependent. Increasing the values of l_2 results increasing model stiffness and yields upper frequencies.

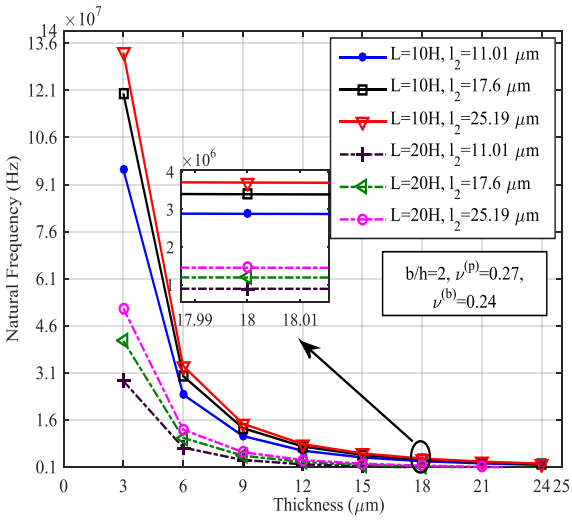

Fig. 6- Effect of natural frequency on the variation of the thickness of micro cantilever beam with different size-dependent

Fig. 7 shows the distribution of the first natural frequency in terms of length to thickness ratio for different values of

length scale parameter l_2.The obtained results in this figure indicate that by increasing the length scale ratio l_2, the natural frequencies of the model increases considerably. It is worth mentioning that decreasing length to thickness parameter follows this trend upward.

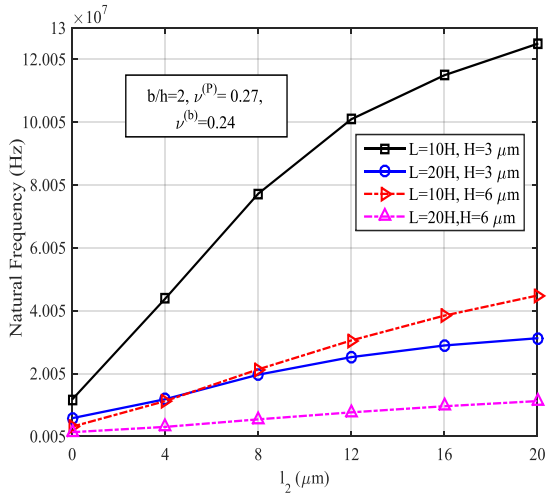

Fig. 7- Distribution of first natural frequencies of sandwich micro-beam in terms of length scale parameter l_2

4-3- Surface effects

The effect of the thickness to length ratio of cantilever micro-beam based on MCST and CT model are considered on the responses of natural frequency in Fig. 8. The effects of various surface residual stress values have been shown. It is observed that the natural frequency increases with the growth of the surface residual stress.

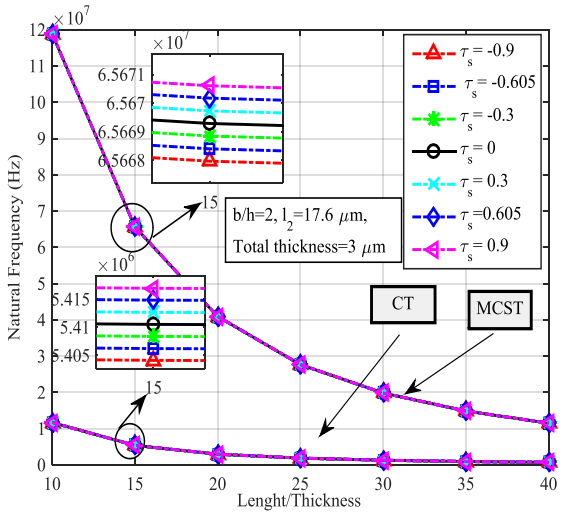

Fig. 8- The natural frequency for micro-beam model versus aspect ratio for different values of surface residual stress based on CT and MCST.

Fig. 9 shows the natural frequency of cantilever micro-beam integrated with piezoelectric layers based on MCST and CT versus aspect ratio for different values of surface elastic modulus. It is concluded that employing surface elastic modulus on the natural frequency is considerable. It is noted that with the increase of the surface elastic modulus terms, the natural frequency of the micro-beam will show a slow growth.

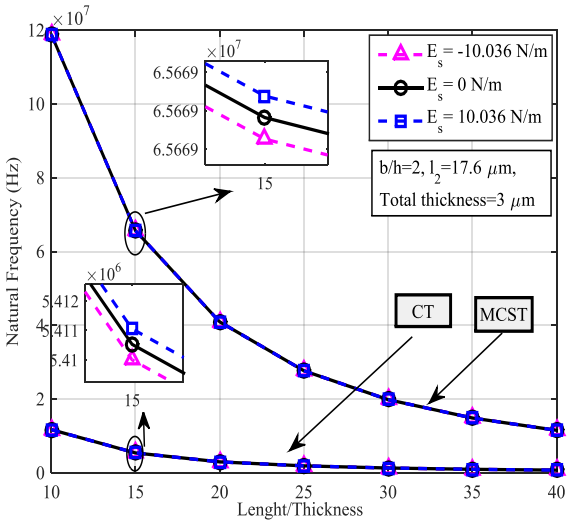

Fig. 9- The natural frequency for micro-beam model versus aspect ratio for different values of surface elastic modulus based on CT and MCST

The values of the different cases of surface effects were defined in Table 2.The influence of different cases on variations of first the natural frequency for the micro cantilever beam model based on MCST is shown in Fig. 10.

In this simulation, the total thickness of the model is assumed to be 3 μm. It is obvious that the stiffness of micro beam increases at lower thickness to length aspect ratios. In other words, it can be concluded that the natural frequency decreases with the growth of the thickness to length aspect ratio. Comparison of the results in Fig. 10 indicates that the surface density can decrease the natural frequencies of model. Also, the effective stiffness of the model can be strengthened by surface elastic modulus and surface residual stress. Hence, the highest natural frequency values were related to case 3, 2 and 1 and the lowest natural frequency belongs to case 6 and 7, respectively. The result shows that there has been a slight influence on the natural frequency with surface piezoelectric constant assumption. It is concluded that employing surface piezoelectric constant on the natural frequency is negligible.

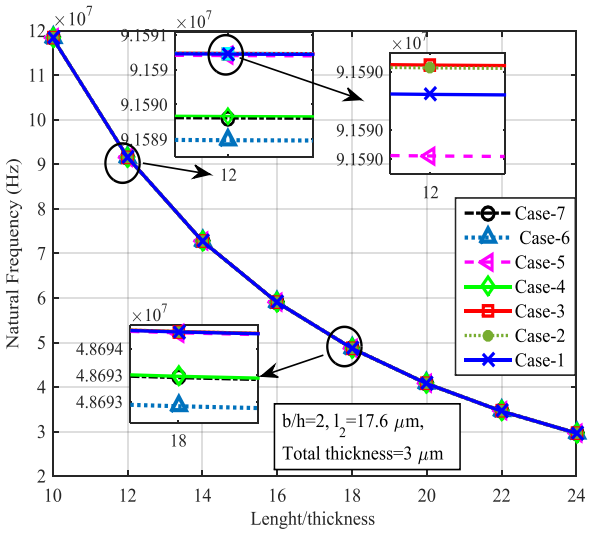

Fig. 10- Variations of the first natural frequencies of micro cantilever beam model based on MCST under different surface effect defined in Table 2.

Table 2 Different cases of surface effect model defined in the work, considering surface elastic modulus, surface residual stress, surface density and surface piezoelectric constant [23, 28].

Case type	Surface effect parameters			
	$\tau^s\ (N/m)$	$E^s(N/m)$	$\rho_s\ (Kg/m^2)$	$e_{31}^s\ (C/m)$
Case-1	0.605	10.036	3.17×10^{-7}	-3×10^{-8}
Case-2	0.605	10.036	0	-3×10^{-8}
Case-3	0.605	10.036	0	0
Case-4	0	10.036	0	0
Case-5	0.605	0	0	0
Case-6	0	0	3.17×10^{-7}	0
Case-7	0	0	0	0

Table 3. illustrates the numerical result of first natural frequency under different surface effect cases for micro cantilever beam integrated with piezoelectric layers based on MCST which have been defined in Table 2.

Table 3. The effect of various surface effect cases on first natural frequency of micro cantilever beam integrated with piezoelectric layers based on MCST for length 42 μ_m

Case type	$\omega_1(Hz)$
Case-1	72762427.62
Case-2	72762437.73
Case-3	72762438.55
Case-4	72761544.7
Case-5	72762410.71
Case-6	72761301.3
Case-7	72761516.51

5 -Conclusion:

In this work, the free vibration analysis of sandwich micro-beam with piezoelectric layers including modified couple stress and surface stress elasticity was presented. The governing equations of motion were obtained based on the variational method. Then, these equations discretized by the GDQ method. Thus, the set of partial differential equations were converted to the set of ordinary differential equations. The results of this study imply to considering the independent material length scale parameter associated symmetric rotation gradients, leads to increase stiffness of model and natural frequency. In addition, it was revealed that surface stress conjunctive with modified couple stress theory predicted natural frequency more accurately than classical model. Also, it was found that natural frequency with considering surface residual stress is greater than other surface effect frequencies. It is observed that natural frequencies increase nonlinearly when the material length scale l_2 value increases.

References:

[1] N. Fleck, G. Muller, M. Ashby, J. Hutchinson, "Strain gradient plasticity: theory and experiment," Acta Metallurgica et Materialia, vol. 42, 1994, pp. 475-487.

[2] J. Stölken, A. Evans, "A microbend test method for measuring the plasticity length scale," Acta Materialia, vol. 46, 1998, pp. 5109-5115.

[3] A.C. Eringen, D. Edelen, "On nonlocal elasticity," International Journal of Engineering Science, vol. 10, 1972, pp. 233-248.

[4] U.B. Ejike, "The plane circular crack problem in the linearized couple-stress theory," International Journal of Engineering Science, vol. 7, 1969, pp. 947-961.

[5] F. Yang, A. Chong, D.C.C. Lam, P. Tong, "Couple stress based strain gradient theory for elasticity," International Journal of Solids and Structures, vol. 39, 2002, pp. 2731-2743.

[6] D.C. Lam, F. Yang, A. Chong, J. Wang, P. Tong, "Experiments and theory in strain gradient elasticity," Journal of the Mechanics and Physics of Solids, vol. 51, 2003, pp. 1477-1508.

[7] S. Park, X. Gao, "Bernoulli–Euler beam model based on a modified couple stress theory," Journal of Micromechanics and Microengineering, vol. 16, 2006, pp. 2355.

[8] S. Kong, S. Zhou, Z. Nie, K. Wang, "The size-dependent natural frequency of Bernoulli–Euler micro-beams," International Journal of Engineering Science, vol. 46, 2008, pp. 427-437.

[9] R.A. Alashti, A. Abolghasemi, "A size-dependent Bernoulli-Euler beam formulation based on a new model of couple stress theory," International Journal of Engineering TRANSACTIONS C, vol. 27, 2014, pp. 951-960.

[10] H. Farokhi, M.H. Ghayesh, M. Amabili, "Nonlinear dynamics of a geometrically imperfect microbeam based on the modified couple stress theory," International Journal of Engineering Science, vol. 68, 2013, pp. 11-23.

[11] B. Akgöz, Ö. Civalek, "Strain gradient elasticity and modified couple stress models for buckling analysis of axially loaded micro-scaled beams," International Journal of Engineering Science, vol. 49, 2011, pp. 1268-1280.

[12] S. Kong, S. Zhou, Z. Nie, K. Wang, "Static and dynamic analysis of micro beams based on strain gradient elasticity theory," International Journal of Engineering Science, vol. 47, 2009, pp. 487-498.

[13] X. Liang, S. Hu, S. Shen, "A new Bernoulli–Euler beam model based on a simplified strain gradient elasticity theory and its applications," Composite Structures, vol. 111, 2014, pp. 317-323.

[14] K. Lazopoulos, A. Lazopoulos, "Bending and buckling of thin strain gradient elastic beams," European Journal of Mechanics-A/Solids, vol. 29, 2010, pp. 837-843.

[15] M.A. Trindade, A. Benjeddou, "Refined sandwich model for the vibration of beams with embedded shear piezoelectric actuators and sensors," Computers & Structures, vol. 86, 2008, pp. 859-869.

[16] M.-R. Ghazavi, G. Rezazadeh, S. Azizi, "Pure parametric excitation of a micro cantilever beam actuated by piezoelectric layers," Applied Mathematical Modelling, vol. 34, 2010, pp. 4196-4207.

[17] S. Sahmani, M. Bahrami, "Size-dependent dynamic stability analysis of microbeams actuated by piezoelectric voltage based on strain gradient elasticity theory," Journal of Mechanical Science and Technology, vol. 29, 2015, pp. 325.

[18] A.G. Arani, M. Abdollahian, R. Kolahchi, "Nonlinear vibration of a nanobeam elastically bonded with a piezoelectric nanobeam via strain gradient theory," International Journal of Mechanical Sciences, vol. 100, 2015, pp. 32-40.

[19] M.E. Gurtin, A.I. Murdoch, "A continuum theory of elastic material surfaces," Archive for rational mechanics and analysis, vol. 57, 1975, pp. 291-323.

[20] Y. Fu, J. Zhang, "Size-dependent pull-in phenomena in electrically actuated nanobeams incorporating surface energies," Applied Mathematical Modelling, vol. 35, 2011, pp. 941-951.

[21] M. Mohammadimehr, M.M. Mohammadi Najafabadi, H. Nasiri, B. Rousta Navi, "Surface stress effects on the free vibration and bending analysis of the nonlocal single-layer graphene sheet embedded in an elastic medium using energy method," Proceedings of the Institution of Mechanical Engineers, Part N: Journal of Nanomaterials, Nanoengineering and Nanosystems, vol. 230, 2016, pp. 148-160.

[22] H.M. Sedighi, A. Koochi, M. Abadyan, "Modeling the size dependent static and dynamic pull-in instability of cantilever nanoactuator based on strain gradient theory," International Journal of Applied Mechanics, vol. 6, 2014, pp. 1450055.

[23] M. Mohammadimehr, H. Mohammadi Hooyeh, H. Afshari, M.R. Salarkia, "Free vibration analysis of double-bonded isotropic piezoelectric Timoshenko microbeam based on strain gradient and surface stress elasticity theories under initial stress using differential quadrature method," Mechanics of Advanced Materials and Structures, vol.24, 2017, pp. 287-303.

[24] M. Keivani, A. Koochi, A. Kanani, M.R. Mardaneh, H.M. Sedighi, M. Abadyan, "Using strain gradient elasticity in conjunction with Gurtin–Murdoch theory for modeling the coupled effects of surface and size phenomena on the instability of narrow nano-switch," Proceedings of the Institution of Mechanical Engineers, Part C: Journal of Mechanical Engineering Science, vol. 231, 2017, pp. 3277-3288.

[25] S.A. Mirkalantari, M. Hashemian, S.A. Eftekhari, D. Toghraie, "Pull-in instability analysis of rectangular nanoplate based on strain gradient theory considering surface stress effects," Physica B: Condensed Matter, vol. 519, 2017, pp. 1-14.

[26] M. Keivani, A. Koochi, H.M. Sedighi, A. Abadian, M. Abadyan, "A Nonlinear Model for Incorporating the Coupled Effects of Surface Energy and Microstructure on the Electromechanical Stability of NEMS," Arabian Journal for Science and Engineering, vol. 41, 2016, pp. 4397-4410.

[27] S. Foroutan, A. Haghshenas, M. Hashemian, S.A. Eftekhari, D. Toghraie, "Spatial buckling analysis of current-carrying nanowires in the presence of a longitudinal magnetic field accounting for both surface and nonlocal effects," Physica E: Low-dimensional Systems and Nanostructures, vol. 97, 2018, pp. 191-205.

[28] K.-M. Hu, W.-M. Zhang, Z.-K. Peng, G. Meng, "Transverse vibrations of mixed-mode cracked nanobeams with surface effect," Journal of Vibration and Acoustics, vol. 138, 2016, pp. 011020.

Appendix:

$$\mathrm{A}_1 = \frac{1}{2} b E^b \left[\frac{h_0^3}{12}\right]$$

$$\mathrm{A}_2 = \frac{1}{2} b E^{(p1)} \left[\frac{\left(\frac{h_0}{2} + h^{(p1)}\right)^3}{3} - \frac{\left(\frac{h_0}{2}\right)^3}{3}\right]$$

$$\mathrm{A}_3 = \frac{1}{2} b E^{(p2)} \left[\frac{\left(-\frac{h_0}{2}\right)^3}{3} - \frac{\left(-\frac{h_0}{2} - h^{(p2)}\right)^3}{3}\right]$$

$$\mathrm{A}_4 = \frac{1}{2} e_{31} b \left[\frac{1}{\beta}\left(\cos\left(\beta\left(\frac{h_0}{2} + h^{(p1)}\right)\right) - \cos\left(\beta\frac{h_0}{2}\right)\right) + \left(\frac{h_0}{2} + h^{(a)}\right)\left(\sin\left(\beta\left(\frac{h_0}{2} + h^{(p1)}\right)\right) - \left(\frac{h_0}{2}\right)\sin\left(\beta\frac{h_0}{2}\right)\right)\right]$$

$$A_5 = \frac{1}{2} e_{31} b \left[\frac{1}{\beta}\left(\cos\left(-\beta\frac{h_0}{2}\right) - \cos\left(\beta\left(-\frac{h_0}{2} - h^{(p2)}\right)\right)\right) - \left(\frac{h_0}{2}\right)\sin\left(-\beta\frac{h_0}{2}\right) + \left(\frac{h_0}{2} + h^{(p2)}\right)\left(\sin\left(\beta\left(-\frac{h_0}{2} - h^{(p2)}\right)\right)\right)\right]$$

$$\mathrm{A}_6 = \left(-\rho^{(p1)} I^{(p1)} - \rho^{(p2)} I^{(p2)} - \rho^{(b)} I^{(b)}\right)$$

$$A_7 = \left(\rho^{(p1)} A^{(p1)} + \rho^{(p2)} A^{(p2)} + \rho^{(b)} A^{(b)}\right)$$

$$A_8 = \frac{1}{2} e_{31} b h^{(p1)}$$

$$A_9 = -\frac{1}{2} \epsilon_{33} \beta b \left[\cos\left(\beta\left(\frac{h_0}{2} + h^{(p1)}\right)\right) - \cos\left(\beta\frac{h_0}{2}\right)\right]$$

$$A_{10} = \frac{1}{2} e_{31} b h^{(p2)}$$

$$A_{11} = -\frac{1}{2}\epsilon_{33}\beta b\left[\cos\left(-\beta\frac{h_0}{2}\right) - \cos\left(\beta\left(-\frac{h_0}{2}-h^{(p2)}\right)\right)\right]$$

$$A_{12} = \mu^{(p2)}l_2^2A^{(p2)}$$

$$A_{13} = \mu^{(p1)}l_2^2A^{(p1)}$$

$$A_{14} = \mu^{(b)}l_2^2A^{(b)}$$

$$B_1^S = E_s^{(b)}\frac{h^2}{4}b$$

$$B_2^S = \frac{1}{2}e_{31}^{s(p1)}b\beta\left(-\frac{h}{2}\right)\cos\left(-\frac{h}{2}\beta\right)$$

$$B_3^S = 2\tau_s^{(p1)}b$$

$$B_4^S = 2\left(-\frac{h_0^3}{24}+\frac{h^3}{24}\right)E_s^{(p1)}$$

$$B_5^S = e_{31}^{s(p1)}\left[\frac{1}{\beta}\cos\left(-\frac{h_0}{2}\beta\right) - \frac{h_0}{2}\sin\left(-\beta\frac{h_0}{2}\right) - \frac{1}{\beta}\cos\left(-\frac{h}{2}\beta\right) + \frac{h}{2}\sin\left(-\beta\frac{h}{2}\right)\right]$$

$$B_6^S = E_s^{(p1)}\frac{h_0^2}{4}b$$

$$B_7^S = \frac{1}{2}e_{31}^{s(a)}(b)\left(-\frac{h_0}{2}\right)\beta\cos\left(-\frac{h_0}{2}\beta\right)$$

$$B_8^S = E_s^{(p1)}b\frac{h_0^2}{2} + E_s^{(b)}\frac{h_0^3}{6}$$

$$B_9^S = 2\tau_s^{(b)}b$$

$$B_{10}^S = E_s^{(p2)}\frac{h^2}{4}b$$

$$B_{11}^S = \frac{1}{2}e_{31}^{s(p2)}b\beta\left(\frac{h}{2}\right)\cos\left(\frac{h}{2}\beta\right)$$

$$B_{12}^S = 2\tau_s^{(p2)}b$$

$$B_{13}^S = e_{31}^{s(p2)}\left[\frac{1}{\beta}\cos\left(\frac{h}{2}\beta\right) + \frac{h}{2}\sin\left(\beta\frac{h}{2}\right) - \frac{1}{\beta}\cos\left(\frac{h_0}{2}\beta\right) - \frac{h_0}{2}\sin\left(\beta\frac{h_0}{2}\right)\right]$$

$$B_{14}^S = 2(-\frac{h^3}{24}+\frac{h_0^3}{24})E_s^{(p2)}$$

$$B_{15}^S = E_s^{(p2)}\frac{h_0^2}{4}b$$

$$B_{16}^S = \frac{1}{2}e_{31}^{s(p2)}b\left(\frac{h_0}{2}\right)\beta\cos\left(\frac{h_0}{2}\beta\right)$$